Supporting information

Na-β-Al_2O_3 stabilized Fe_2O_3 oxygen carriers for chemical looping water splitting: correlating structure with redox stability

*Nur Sena Yüzbasi [a], Andac Armutlulu [a], Thomas Huthwelker [b], Paula M. Abdala *, [a], Christoph R. Müller *, [a]*

[a] Laboratory of Energy Science and Engineering, ETH Zurich, Leonhardstrasse 27, 8092, Zurich, Switzerland

[b] PHOENIX X07MA/B Beamline, Paul Scherrer Institut, 5232, Villigen PSI, Switzerland

*Corresponding authors: abdalap@ethz.ch, muelchri@ethz.ch

Table S1: Weight-based composition, surface areas, pore volumes and particle diameters of the materials calcined at 900 °C.

		FeAl	FeAlNa1	FeAlNa5
Nominal weight compositions	**Fe_2O_3 (wt. %)**	75	76	76
	Al_2O_3 (wt. %)	25	23	19
	Na_2O (wt. %)	-	1	5
	Al_2O_3:Fe_2O_3 ratio	0.33	0.30	0.33
Weight-based compositions calculated from EDX	**Fe_2O_3 (wt. %)**	77	76.4	73.8
	Al_2O_3 (wt. %)	23	22.5	21.9
	Na_2O (wt. %)		1.1	4.3
	Al_2O_3:Fe_2O_3 ratio	0.30	0.30	0.33
Molar ratios calculated from EDX	**Fe**	0.96	0.95	0.94
	Al	0.44	0.42	0.42
	Na	-	0.03	0.14
Surface Area [m^2/g]		9	17	11
Pore Volume [cm^3/g]		0.1	0.19	0.13
Average particle size [nm]		112 ± 35	107 ± 25	100 ± 27

Table S2: Phase composition and cell parameters determined by Rietveld refinement of the XRD data of the calcined oxygen carriers.[a]

		a [Å]	b [Å]	c [Å]	Cell volume [Å^3]	Phase content [wt %]	Rp	Rwp	Rexp
FeAl	**Fe_2O_3**	5.0169(1)	5.0169(1)	13.6849(5)	298.29 (1)	73(1)	6.35	9.07	3.78
	Al_2O_3	4.7851(3)	4.7851(3)	13.054(1)	258.86(3)	27(1)			
FeAlNa1	**Fe_2O_3**	5.0173(1)	5.0173(1)	13.6898(5)	298.46(2)	77(1)	5.37	7.19	3.79
	Al_2O_3	4.7829(2)	4.7829(2)	13.053(1)	258.59(3)	23(1)			
FeAlNa5	**Fe_2O_3**	5.0181(1)	5.0181(1)	13.6867(1)	298.48(1)	82(1)	7.07	9.55	3.79
	Al_2O_3	4.782 (1)	4.782(1)	13.047(6)	258.4(1)	3(1)			
	$NaAl_{11}O_{17}$	5.6385(8)	5.6385(8)	22.816(6)	628.2(2)	15(1)			

[a] Fe_2O_3 phase: *R-3c* space group, with atomic positions as reported in [1], Al_2O_3 phase: *R-3c* space group, with atomic positions as reported in [2] and Na-β-Al_2O_3: *$P6_3/mmc$* space group with atomic positions as reported in [3]

1. *P. Schouwink, L. Dubrovinsky, K. Glazyrin, M. Merlini, M. Hanfland, T. Pippinger and R. Miletich, American Mineralogist, 2011, **96**, 1781-1786.*
2. *S. Kondo, K. Tateishi and N. Ishizawa, Japanese Journal of Applied Physics, 2008, **47**, 616.*
3. *N. Zhu, F. Guo, S. Yan, L. Chen and A. Li, Acta Chimica Sinica, 1992, **50**, 527-532.*

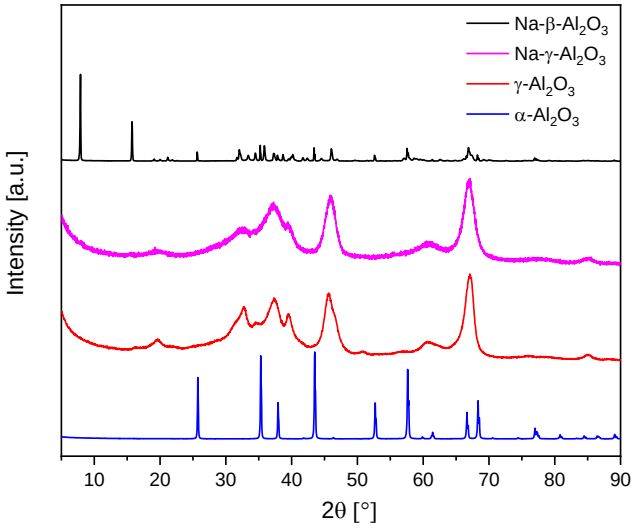

Figure S1: XRD patterns of the reference materials: γ-Al_2O_3, α-Al_2O_3, Na-γ-Al_2O_3 and Na-β-Al_2O_3.

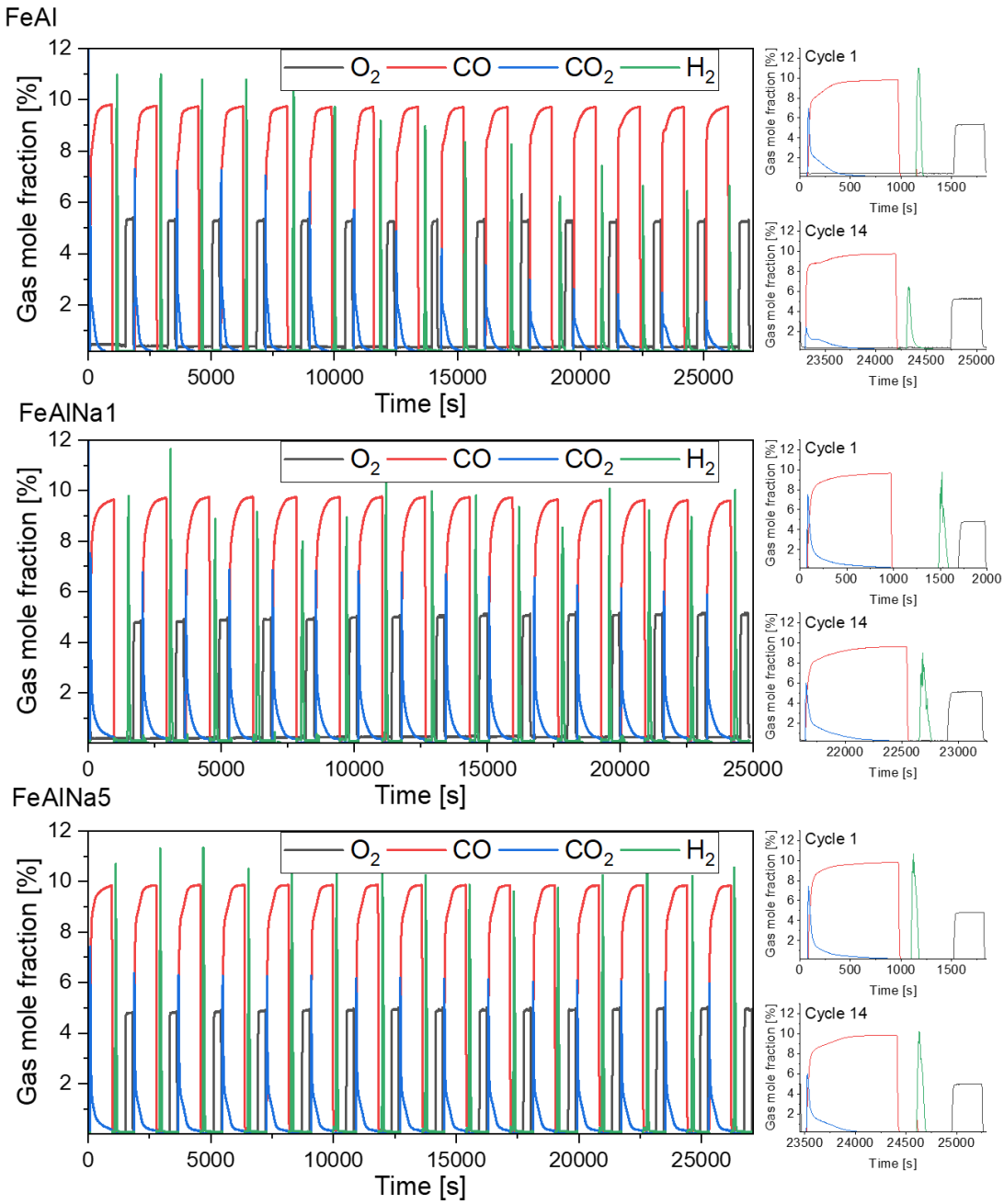

Figure S2: Concentration profiles of the off gases during redox cycling for the different oxygen carriers investigated. Insets show cycle 1 and 14.

The conversion of CO during reduction, Xco, is plotted in Figure S3b and was calculated from the quantity of CO consumed according to:

$$Xco = \frac{m_{CO}}{x_{oc} m_{oc}} . \left(\frac{M_{Fe_2O_3}}{M_{CO}} . \frac{1}{3} \right) \quad \text{(S1)}$$

where m_{co} is the mass of CO consumed, m_{oc} is the mass of the oxygen carrier, x_{oc} is the mass fraction of Fe_2O_3 in the oxygen carrier and $M_{Fe_2O_3}$ and M_{CO} are the molecular weights of Fe_2O_3 and CO, respectively. 1/3 is the stoichiometric ratio of Fe_2O_3/CO during reduction.

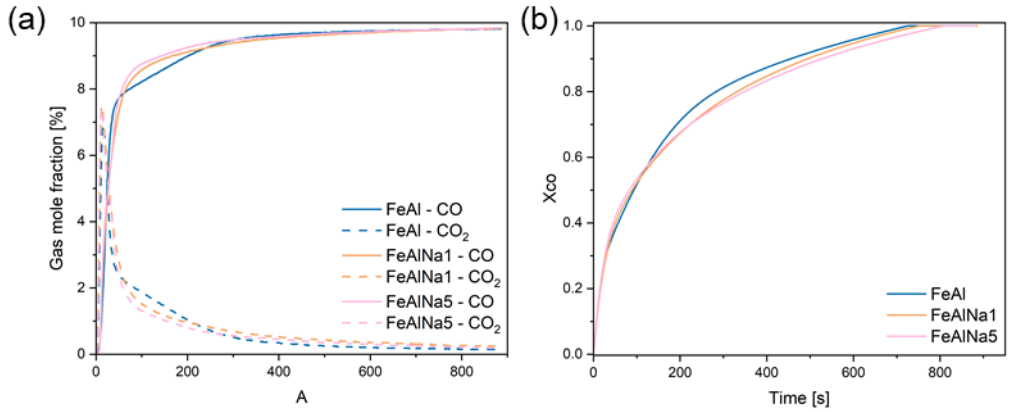

Figure S3: Reduction of the different oxygen carriers in the first cycle: (a) Concentration profiles of the off gases and (b) conversion of the oxygen carriers.

To compare the reduction characteristics of the different oxygen carriers, we performed temperature programmed reduction (TPR) experiments (Figure S4). In a typical test, ~ 30 mg of the oxygen carrier was heated up in 10 vol.% CO (balance N_2) or 10 vol.% H_2 (balance N_2) from 25 to 800 °C using a temperature ramp of 10 °C/min. Subsequently the oxygen carriers were held at 800 °C for 2 h. Our CO-TPR (Figure S4a) and H_2-TPR (Figure S4b) experiments indicate that the reduction of the oxygen carriers is slower in CO compared to H_2. Additionally, Figure S4c plots the H_2-consumption during H_2-TPR. There is no significant difference in the reduction characteristics of the oxygen carriers studied; in line with the findings obtained from the analysis of the off gas composition in the redox cycling experiments (Figure S3).

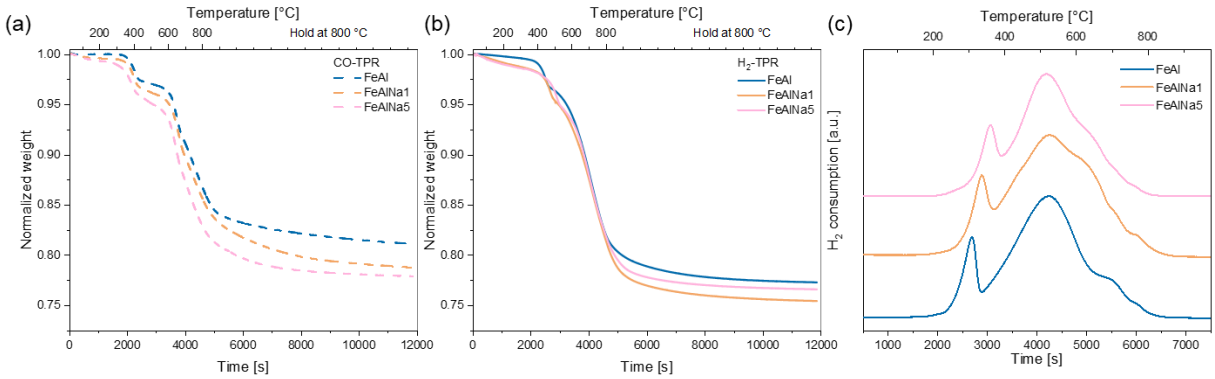

Figure S4: Temperature-programmed reduction experiments: (a) CO-TPR, (b) H_2-TPR and (c) H_2-consumption during H_2-TPR.

To explore the effect of the addition of sodium and cycle number on the water splitting kinetics, the conversion, X_{H_2}, during steam oxidation was calculated from the quantity of H_2 produced:

$$X_{H_2} = \frac{m_{H_2}}{x_{oc} m_{oc}} . \left(\frac{M_{Fe_2O_3}}{M_{H_2}} . \frac{3}{8} \right) \quad \text{(S2)}$$

where m_{H_2} is the mass of H_2 produced, m_{oc} is the mass of the oxygen carrier, x_{oc} is the mass fraction of Fe_2O_3 in the oxygen carrier and $M_{Fe_2O_3}$ and M_{H_2} are the molecular weights of Fe_2O_3 and H_2, respectively. 3/8 is the stoichiometric ratio of Fe_2O_3/H_2 during oxidation.

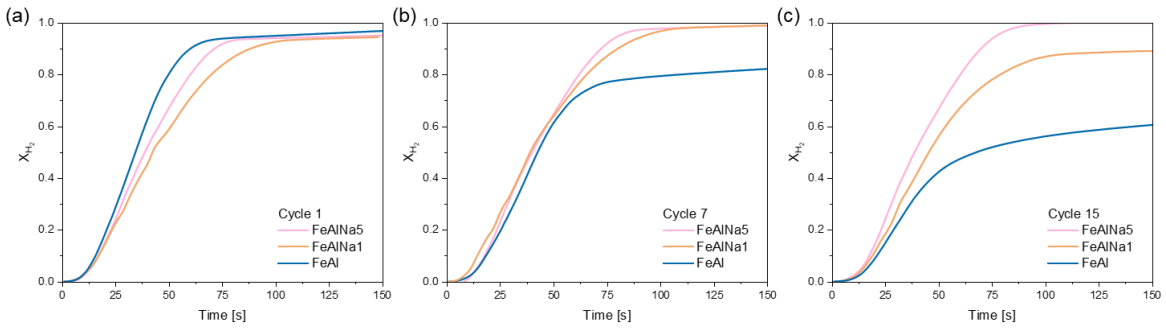

Figure S5: Effect of cycle number on the fractional conversion of the oxygen carriers in (a) cycle 1, (b) cycle 7 and (c) cycle 15 during steam oxidation.

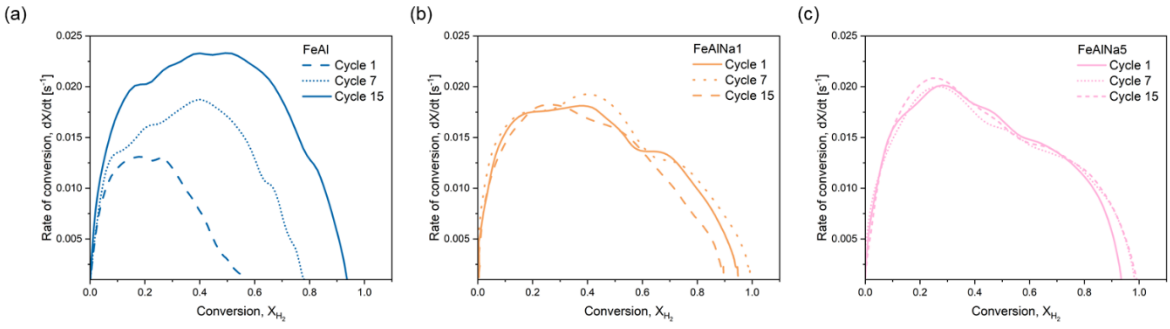

Figure S6: Rate of conversion as a function of total conversion of (a) FeAl, (b) FeAlNa1 and (c) FeAlNa5 during steam oxidation.

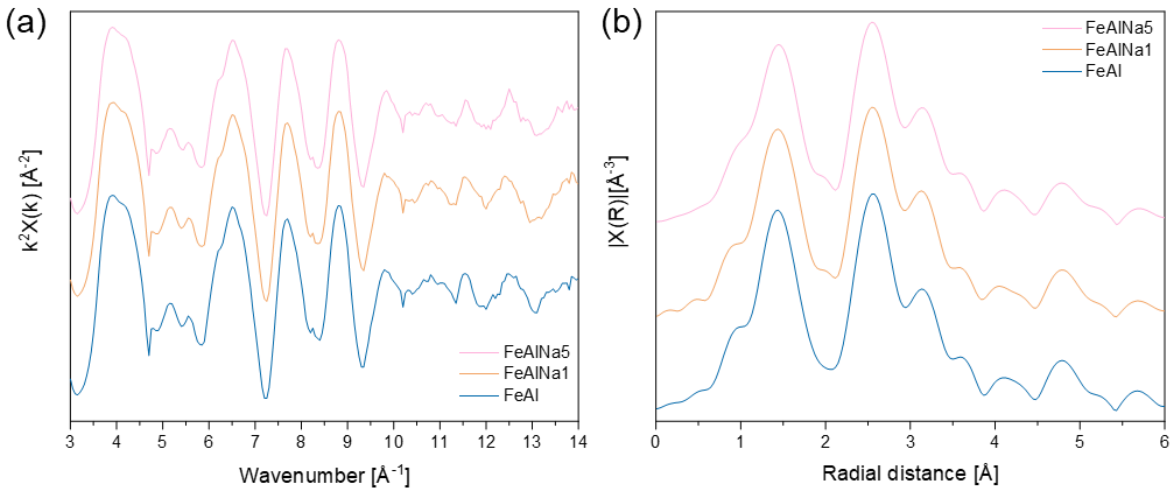

Figure S7: (a) k^2–weighted EXAFS spectra and (b) Fourier transformed EXAFS functions (k^2–weighted) of the calcined oxygen carriers measured at the Fe K-edge.

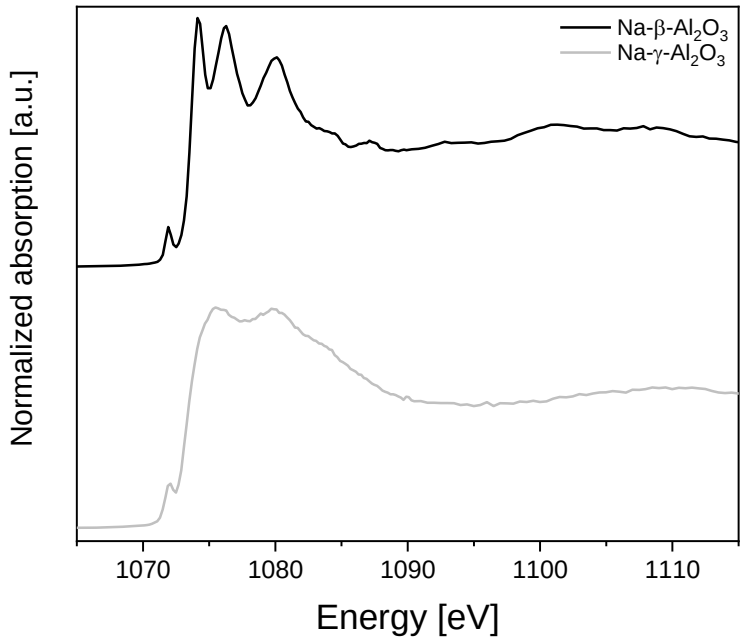

Figure S8: XANES spectra at the Na K-edge of the reference materials

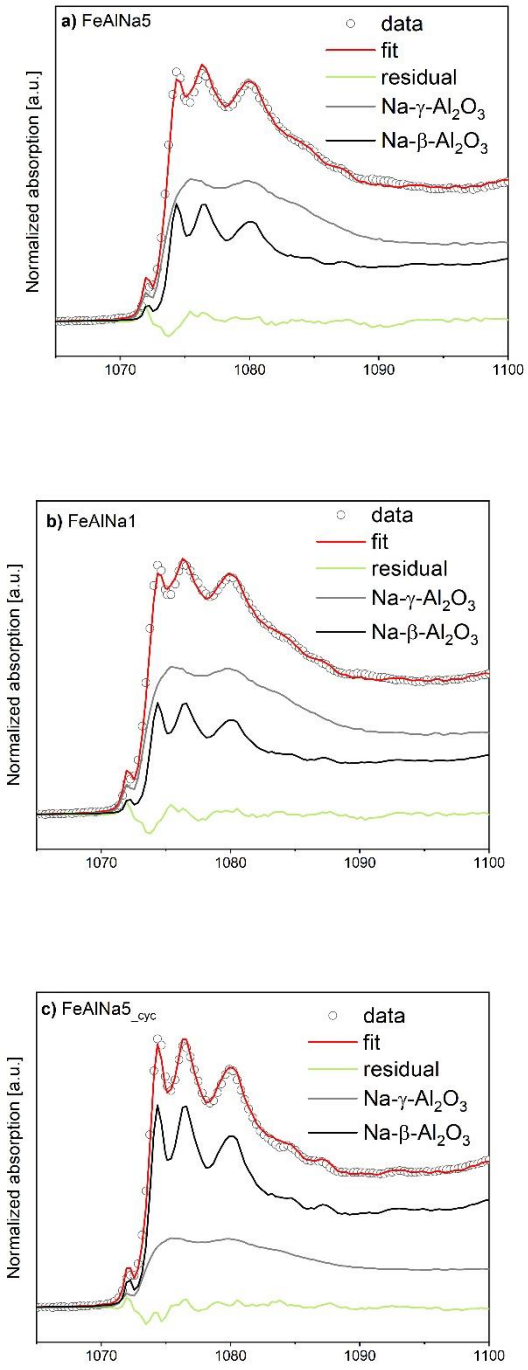

Figure S9: Linear combination fitting analysis of the Na K-edge XANES spectra of FeAlNa5, FeAlNa1 and FeAlNa5$_{_cyc}$ using Na-β-Al_2O_3 and Na-γ-Al_2O_3 as references.

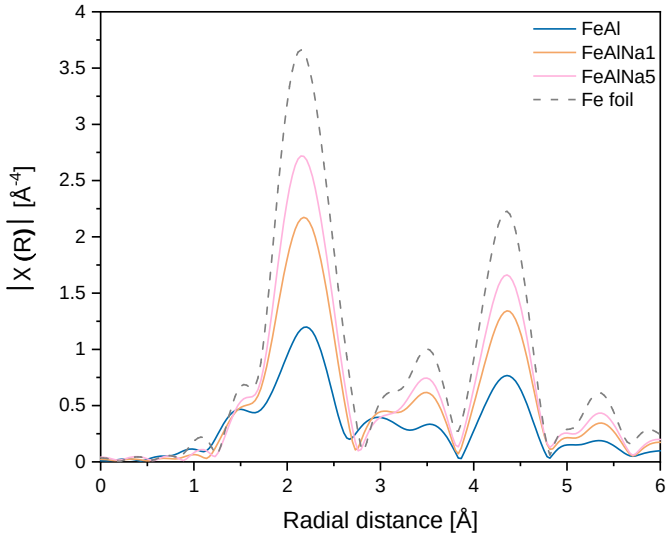

Figure S10: FT-EXAFS functions (k^3–weighted) at the Fe K-edge of the cycled oxygen carriers.

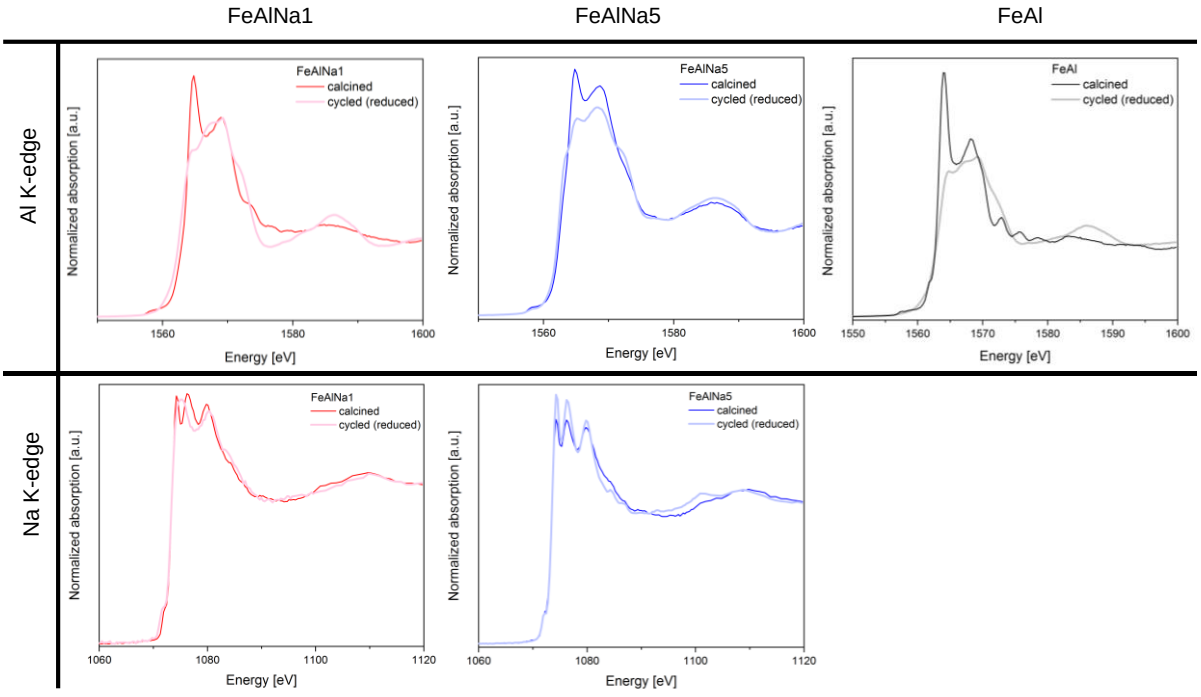

Figure S11: Comparison of the XANES spectra at the Na and Al K-edges of the materials before and after cyclic redox tests (15 cycles, reduced state).

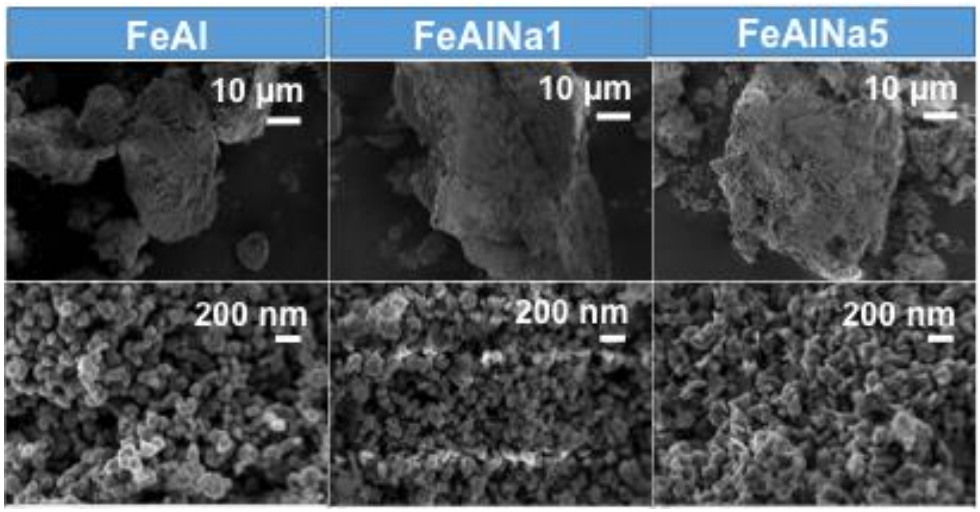

Figure S12: Electron micrographs of the calcined oxygen carriers.

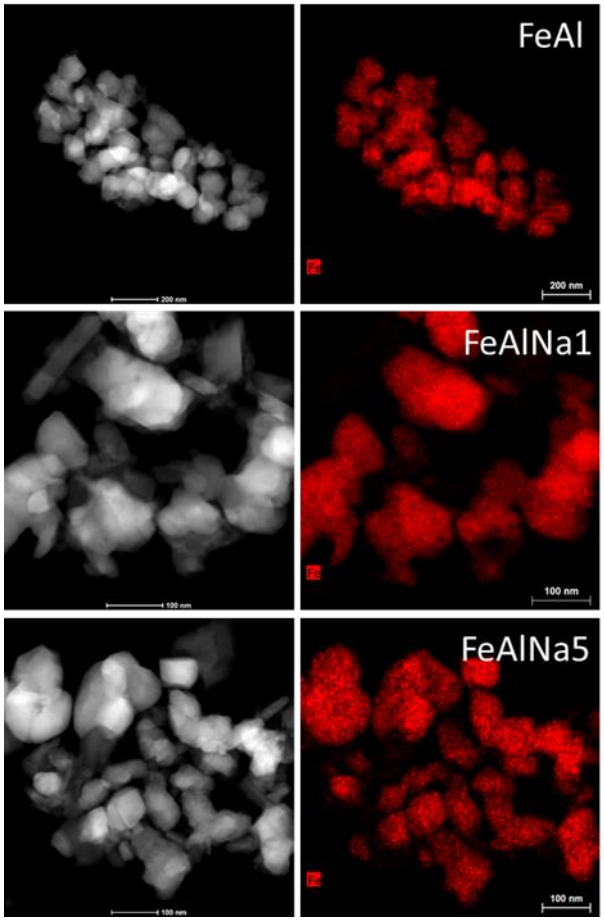

Figure S13: HAADF images of the calcined oxygen carriers and elemental maps of iron (STEM−EDX).

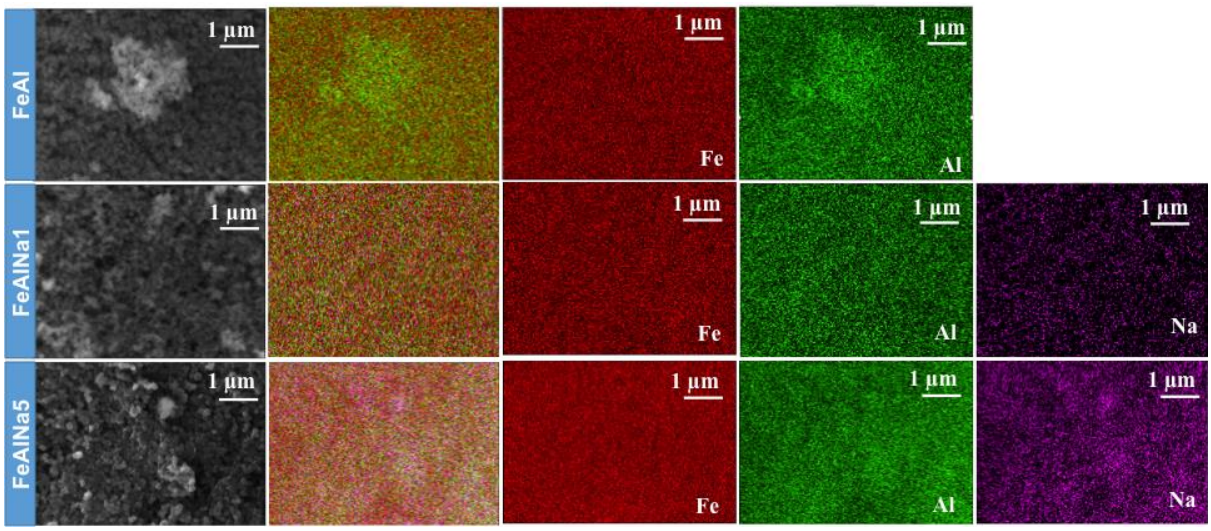

Figure S14: SEM/EDX maps of the calcined materials.

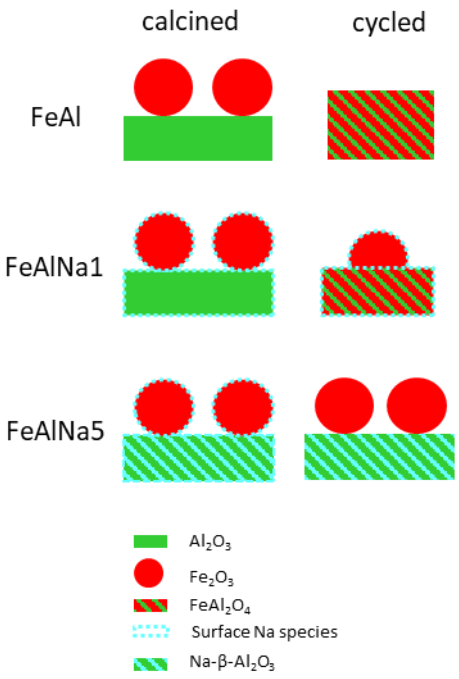

Figure S15: Schematic representation of the phase evolution during redox cycling of FeAl, FeAlNa1 and FeAlNa5.

SEM images of the cycled materials after reduction (in 10 vol. % CO in N_2) and subsequent re-oxidation (in 23 vol. % H_2O in N_2 followed by 5 vol. % O_2 in N_2) are given in Figure S9. SEM images indicate that the oxygen carriers that showed a poor cyclic redox performance (FeAl and FeAlNa1) sintered after having been exposed to 15 redox cycles. The degree of sintering in FeAlNa5 was lower than that in FeAl and FeAlNa1 (over 15 redox cycles).

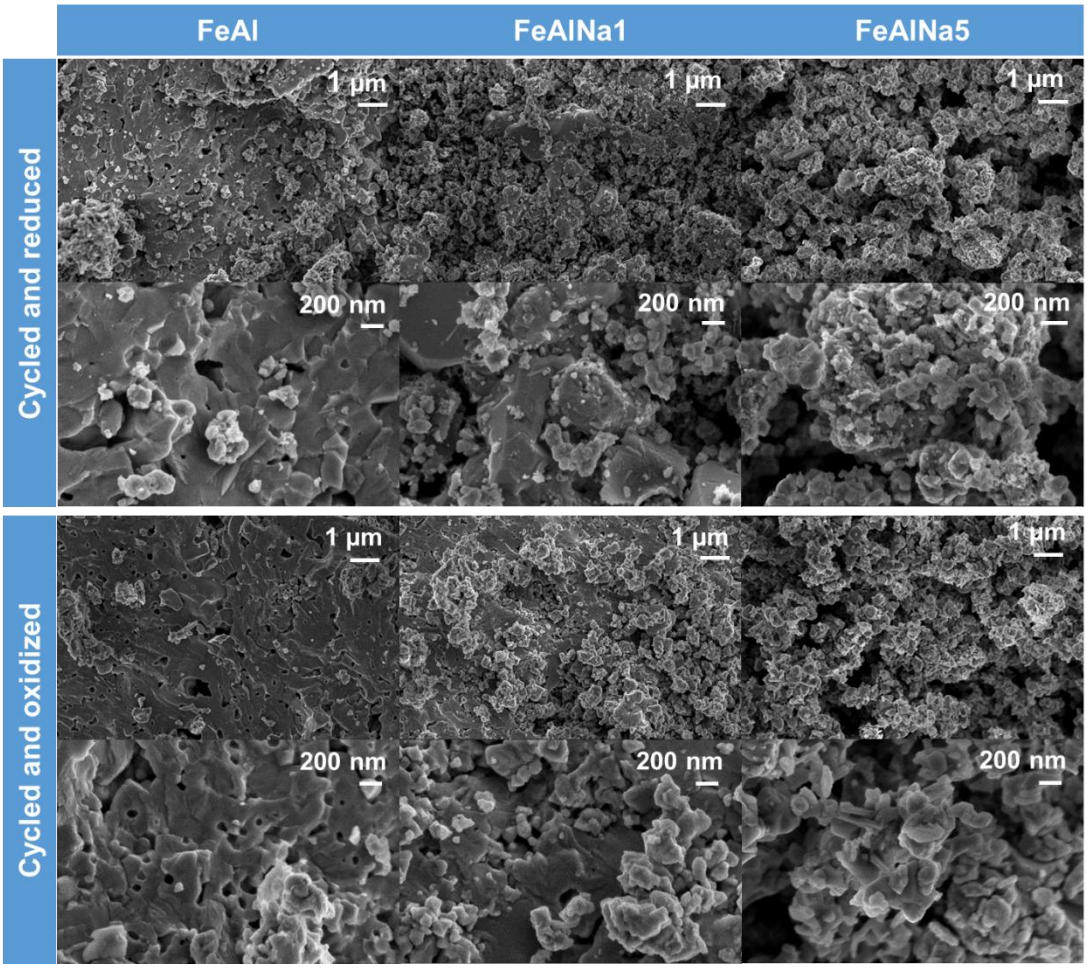

Figure S16: SEM of the cycled (reduced and oxidized states) oxygen carriers after being subjected to 15 redox cycles in a fixed bed.

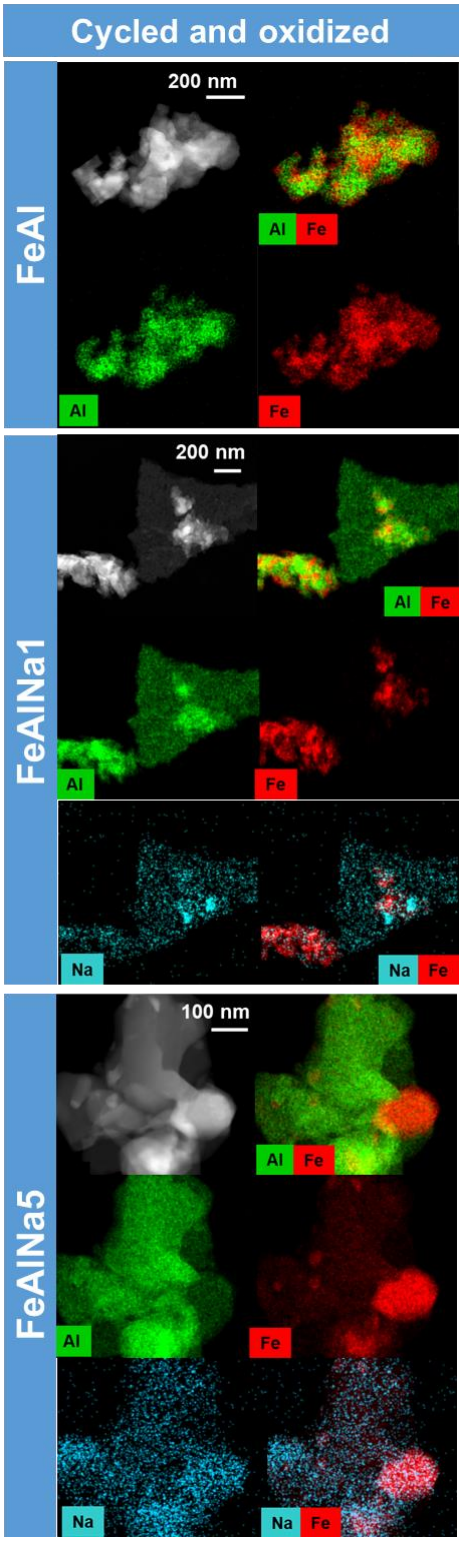

Figure S17: HAADF images and elemental mapping of the cycled oxygen carriers (15 redox cycles, oxidation step); H_2O/N_2 exposure followed by O_2/N_2).